Kinetics and Thermodynamics of the Molecular Mechanism of the Reductive Half-Reaction of Xanthine Oxidase

Madhu Sudan Mondal and Samaresh Mitra*

Chemical Physics Group, Tata Institute of Fundamental Research, Homi Bhabha Road, Bombay 400 005, India

Received January 5, 1994; Revised Manuscript Received June 23, 1994®

ABSTRACT: The kinetics and thermodynamics of the reductive half-reaction of xanthine oxidase with xanthine as substrate have been investigated by stopped-flow kinetic measurements. The temperature dependence of the steady-state and transient kinetics of the reductive half-reaction reveals the existence of at least three molecular intermediates during this half-reaction. All the microscopic rate constants and the thermodynamic activation parameters of the elementary steps of the reductive half-reaction have been determined for the first time. The microscopic rate constants and the thermodynamic activation parameters of the individual steps show wide variations in their magnitudes. The present work provides the most detailed and incisive description of the reaction of xanthine oxidase with its physiological substrate xanthine.

Xanthine oxidase (xanthine:oxygen oxidoreductase, EC 1.2.3.2) is a complex metallo–flavo enzyme with two independent subunits each containing four redox centers: a molybdenum(VI) center; two iron–sulfur (2Fe-2S) clusters, called Fe-S I and Fe-S II; and a flavin adenine dinucleotide (FAD) unit (Bray, 1975, 1988; Hille & Massey, 1985). Xanthine oxidase (XO) catalyzes the oxidation of xanthine in the presence of oxygen to form uric acid, and in the process, hydrogen peroxide or superoxide radical is formed from oxygen. The steady-state conversion reaction of xanthine to uric acid by the oxidized form of the enzyme is known as the reductive half-reaction, while the conversion of oxygen to hydrogen peroxide by the reduced enzyme is known as the oxidative half-reaction. The molybdenum cofactor of the enzyme consists of a molybdenum pterin ring, and the molybdenum atom is bonded to a sulfur atom by a double bond (Mo=S). The presence of a sulfur atom has been shown to be catalytically important (Kramer *et al.*, 1987; Wilson *et al.*, 1991), as it takes part in simultaneous nucleophile–hydride transfer during the reductive half-reaction, making partial negative charge in the substrate, which helps the formation of uric acid (Skibo *et al.*, 1987). The reductive half-reaction takes place at the molybdenum center of the enzyme (Bray *et al.*, 1964; Hille *et al.*, 1989). Xanthine transfers two electrons to the molybdenum atom and reduces the enzyme chromophores, resulting in a decrease of the absorbance in the optical spectrum. During the reductive half-reaction, intramolecular electron transfer (ET) takes place within four redox centers of the enzyme (Olson *et al.*, 1974a,b). The steady-state kinetics of the reaction of XO with various substrates has been studied extensively (Bunting & Gunasekara, 1982; Morpeth, 1983; Skibo, 1986; Skibo *et al.*, 1987; Escribano *et al.*, 1988; D'Ardenne & Edmondson, 1990; Hille & Massey, 1991; Rubbo *et al.*, 1991; Radi *et al.*, 1992) and so has the reductive half-reaction of XO (Olson *et al.*, 1974a,b; Davis *et al.*, 1982, 1984; McWhirter & Hille, 1991; Hille & Massey, 1991; Kim & Hille, 1993). Olson *et al.* (1974b) studied the steady-state and transient kinetics of the reaction of xanthine with XO and suggested a two-step breakdown of the enzyme–substrate complex. The difficulty in detecting the intermediates of the reaction of xanthine with XO is due mainly to their very rapid formation. Skibo *et al.* (1987) have studied the steady-state kinetics of the reaction of XO with quinazoline and have suggested a three-intermediate mechanism of the reductive half-reaction. The steady-state and reductive half-reaction studies of XO with 2-hydroxy-6-methylpurine as substrate have been reported by McWhirter and Hille (1991), which also show the existence of three intermediates. Kim and Hille (1993) showed the existence of three intermediates during the reductive half-reaction with xanthine as substrate. Two of these intermediates differ only in the oxidation state of the molybdenum atom. Xanthine is the physiological substrate for XO. Despite several previous studies, the mechanism of the reductive half-reaction involving different microscopic rate constants and their thermodynamic processes throughout the individual steps of the half-reaction is not yet fully understood, nor is there any kinetic and thermodynamic characterization of more than two intermediates in the molecular mechanism of the reductive half-reaction of XO with xanthine as substrate. The need for an understanding of these aspects of the reductive half-reaction has led us to the present detailed study of the reaction of XO with xanthine.

We have used the rate of the reduction of enzyme chromophores by xanthine as a probe for determining the binding and kinetic parameters of the intermediate molecular complexes. The effect of temperature on the steady-state and reductive half-reactions has been studied to detect the intermediates involved and to determine the kinetic and thermodynamic parameters of elementary reactions. Our results suggest that there are at least three intermediates observable during the reductive half-reaction of XO when xanthine is used as substrate. The kinetics and thermodynamics involved with these intermediates have been investigated. The study allows us to construct an energy diagram of the species involved in the reductive half-reaction of XO with xanthine.

MATERIALS AND METHODS

Fresh unpasteurized cow's milk was obtained from Aarey Milk Colony, Goregaon, Bombay. XO was isolated by the reported procedure (Massy *et al.*, 1969). The activity of the enzyme was measured spectrophotometrically by monitoring the formation of uric acid from xanthine at 295 nm. The

* For correspondence. email address: smitra@tifrvax.bitnet. Fax No.: +91-22-215-2110 or +91-22-215-2181.

® Abstract published in *Advance ACS Abstracts,* August 1, 1994.

0006-2960/94/0433-10305$04.50/0

calculated AFR (activity to flavin ratio) value of the enzyme was in the range of 100–120 which corresponds to 45–55% functional enzyme (Edmondson *et al.*, 1972). The concentration of the enzyme was determined spectrophotometrically by using the molar extinction coefficient of the enzyme as 37 800 M^{-1} cm^{-1} at 450 nm (Massey *et al.*, 1969).

Analytical grade buffers were used. The experiments were done in 100 mM NaH_2PO_4 buffer, pH 7.1.

The oxygen concentration in the sample was measured by an oxygen electrode. The concentration of oxygen in the sample and buffer was increased by purging with high-quality oxygen gas. The conversion reaction of NADH to NAD catalyzed by submitochondrial particles was used for standardizing the electrode. All spectrophotometric experiments were performed on a Shimadzu UV-2100 spectrophotometer.

The stopped-flow kinetic experiments were performed on a Biologic-made (Instruments de Laboratories) stopped-flow machine (SFM3) with three microprocessor-controlled (MPS51) machined syringes. Measurements were done spectrophotometrically by monitoring the wavelength of interest. For the steady-state studies, the syringes were loaded with oxygen-purged samples. The temperature of the syringe reservoir was maintained within ±0.5 °C using a circulating water bath. Sufficient time was allowed to reach each desired temperature. The transient kinetic studies were performed by loading the argon-purged anaerobic samples. The experiments were performed within 2 h of loading the samples. Two syringes were used for mixing the samples. Whenever necessary, the samples were properly diluted using buffer from the third syringe. The data for the rapid kinetics were analyzed from the exponential fitting using Biologic-developed software.

Steady-State Kinetics. The ping-pong mechanism for the steady-state formation of uric acid from xanthine catalyzed by XO can be represented by considering the two independent half-reactions (Hille & Massey, 1991). These reactions can be described by considering the model that xanthine binds to XO very rapidly, forming an enzyme–substrate complex, which subsequently breaks down to the product uric acid by the transfer of two electrons at a comparatively lower rate (Olson *et al.*, 1974b). The mechanism of the reactions is given as (Hille & Massey, 1991)

reductive half-reaction

$$(XO)_{ox} + Xan \underset{k_{-1}}{\overset{k_1}{\rightleftharpoons}} (XO)_{ox}\cdot Xan \xrightarrow{k_2} (XO)_{red} + \text{urate} \quad (1)$$

oxidative half-reaction

$$(XO)_{red} + O_2 \underset{k_{-3}}{\overset{k_3}{\rightleftharpoons}} (XO)_{red}\cdot O_2 \xrightarrow{k_4} (XO)_{ox} + H_2O_2 \text{ (or } O_2^-) \quad (2)$$

The following steady-state rate equation can be derived from the above reaction scheme using the general procedure of King and Altman (1956) (Radi *et al.*, 1992):

$$\gamma_0 = \frac{V_{max}[Xan]_0}{\left(1 + \frac{K_m^{O_2}}{[O_2]_0}\right)\left([Xan]_0 + \frac{K_m^{Xan}}{1 + \frac{K_m^{O_2}}{[O_2]_0}}\right)^{-1}} \quad (3)$$

where

$$V_{max} = \frac{k_2k_4E_0}{k_2 + k_4},\ K_m^{Xan} = \frac{k_4(k_{-1} + k_2)}{k_1(k_2 + k_4)},\ K_m^{O_2} = \frac{k_2(k_{-3} + k_4)}{k_3(k_2 + k_4)}$$

γ_0 is the initial steady-state rate for the conversion of xanthine to uric acid. K_m^{Xan} and $K_m^{O_2}$ are the apparent Michaelis constants for xanthine and uric acid, respectively. V_{max} is the maximum velocity for the overall steady-state turnover of the enzyme. $[Xan]_0$, $[O_2]_0$, and E_0 are the initial concentrations of xanthine, oxygen, and XO, respectively. Under the condition $[O_2]_0 \gg K_mO^2$, eq 3 can be written as

$$\frac{1}{\gamma_0} = \frac{1}{V_{max}} + \frac{K_m^{Xan}}{V_{max}}\frac{1}{[Xan]_0} \quad (4)$$

A plot of $1/\gamma_0$ vs $1/[Xan]_0$ is a straight line, which determines values of K_m^{Xan} and V_{max}.

Transient Kinetics. The reductive half-reaction of XO with xanthine can be monitored anaerobically by observing the enzyme absorbance in the visible region. The measurements of this half-reaction show a monophasic exponential decrease in absorbance, indicating that only the overall rate of the reductive half-reaction can be measured and the substrate binding process is too fast to be observed on this time scale. The pseudo-first-order rate constant (K_{obs}) of the reductive half-reaction of the enzyme can then be given as below (Olson *et al.*, 1974a,b; Davis *et al.*, 1984):

$$\frac{1}{K_{obs}} = \frac{K_D}{k_2}\frac{1}{[Xan]_0} + \frac{1}{k_2} \qquad K_D = \frac{k_{-1}}{k_1} \quad (5)$$

A plot of K_{obs}^{-1} against $[Xan]_0^{-1}$ would allow determination of the dissociation constant (K_D) and k_2.

Determination of Microscopic Rate Constants. From eq 3, we can write

$$\frac{K_m^{Xan}}{V_{max}} = \frac{(k_2 + k_{-1})}{k_1k_2E_0} \quad (6)$$

Combining with eq 5, eq 6 can be rearranged to

$$k_1 = \frac{k_2}{k_2E_0\left(\frac{K_m^{Xan}}{V_{max}}\right) - K_D} \quad (7)$$

The values of K_D (k_{-1}/k_1) and k_2 are known from eq 5 and K_m^{Xan} and V_{max} from eq 4. Thus, eq 7 can be used to obtain the value of k_1. Substitution of k_1 in eq 5 would then give k_{-1}.

Olson *et al.* (1974b) have suggested a two-step breakdown of the enzyme–substrate complex of the reductive half-reaction (eq 1) which considers the existence of the enzyme–product complex as intermediate. This conversion can be represented as (Olson *et al.*, 1974b)

$$(XO)_{ox}\cdot Xan \xrightarrow{k_2'} (XO)_{red}\cdot \text{urate} \xrightarrow{k_2''} (XO)_{red} + \text{urate} \quad (8)$$

Thus the rate constant value k_2 can be given as (Hille & Massey, 1991)

$$k_2 = \frac{k_2'k_2''}{k_2' + k_2''} \text{ or } \frac{1}{k_2} = \frac{1}{k_2'} + \frac{1}{k_2''} \quad (9)$$

The Arrhenius equation ($k = A\exp(-E/RT)$) for the microscopic rate constant can be introduced into eq 9 to obtain an expression for the temperature dependence of the rate constant due to the breakdown of the enzyme–substrate complex. The expression can be written as

$$\frac{1}{k_2} = \frac{1}{A_2'}\exp\left(\frac{E_2'}{RT}\right) + \frac{1}{A_2''}\exp\left(\frac{E_2''}{RT}\right) \quad (10)$$

where A_2' and A_2'' are the frequency factors for the corresponding individual reactions. E_2' and E_2'' are the corresponding activation energies. The temperature dependence of k_2 can be fitted to eq 10 to obtain A_2', A_2'', E_2', and E_2'', which allow the determination of the rate constant values k_2' and k_2'' with the help of the Arrhenius equation.

Determination of Thermodynamic Activation Parameters. Since all the microscopic rate constants (k_1, k_{-1}, k_2', and k_2'') for the reductive half-reaction can be calculated by methods described above, the temperature dependence of the steady-state and transient experiments can be used to calculate the enthalpy ($\Delta H^{\ddagger}$), free energy ($\Delta G^{\ddagger}$), and entropy ($\Delta S^{\ddagger}$) of activation of the individual steps of the enzymatic reactions. The equations relating these thermodynamic parameters are

$$\Delta H^{\ddagger} = E_{act} + RT \quad (11)$$

$$k = \frac{k_B T}{h}\exp\left(\frac{-\Delta G^{\ddagger}}{RT}\right) \quad (12)$$

or

$$k = \frac{k_B T}{h}\exp\left(\frac{\Delta S^{\ddagger}}{R}\right)\exp\left(\frac{-\Delta H^{\ddagger}}{RT}\right) \quad (13)$$

where k_B and h are the Boltzmann constant and Planck's constant, respectively. The thermodynamic parameter for the binding of xanthine to XO was calculated from the van't Hoff equation given as

$$\log K_D = \left(\frac{-\Delta H}{2.303RT}\right) + \frac{\Delta S}{R} \quad (14)$$

$$\Delta G = \Delta H - T\Delta S \quad (15)$$

RESULTS

Steady-State Measurements of the Reaction of XO with Xanthine. The steady-state measurements of XO-catalyzed oxidation of xanthine to uric acid were carried out between 14 and 42 °C by monitoring the increase of uric acid absorption at 295 nm. The oxygen concentration was kept constant at 515 μM for all individual experiments; the oxygen concentration is thus about 10 times larger than its Michaelis constants ($K_m^{O_2}$ = 50 μM) (Massey *et al.*, 1969; Olson *et al.*, 1974a). The higher concentration of oxygen simplifies eq 3 (in the limit of $[O_2] \gg K_m^{O_2}$) and makes the analysis of the experimental data easier (see eq 4). The steady-state production of uric acid with time was found to increase with the increase in the concentration of xanthine (plot is not shown). The Lineweaver–Burk (LB) (Lineweaver & Burk, 1934) plot of the steady-state kinetics in this temperature range is shown in Figure 1. The straight line behavior of the experimental results in Figure 1 is consistent with eq 4 under the experimental condition $[O_2] \gg K_m^{O_2}$. By fitting the data to eq 4, K_m^{Xan} and V_{max} were calculated at different temperatures. These values are listed in Table 1. Our value of K_m^{Xan} at 25 °C (4 μM) is in agreement with that reported earlier (Olson *et al.*, 1974a; Escribano *et al.*, 1988; Morpeth, 1983; Jezewska, 1973; Hille & Massey, 1991). A logarithmic plot of K_m^{Xan} against inverse temperature shows a nonlinear behavior with K_m^{Xan} being minimum at about 25 °C (Figure 2A). The nonlinear dependence of K_m^{Xan} on temperature is, however, expected from eq 3, since K_m^{Xan} is composed of linear combinations of the microscopic rate constants which are individually related

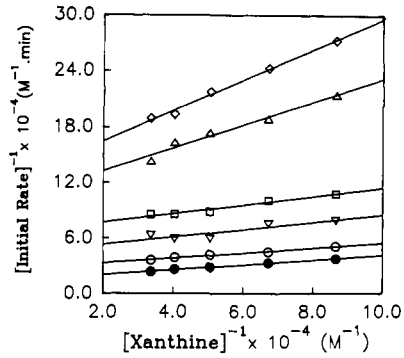

FIGURE 1: Lineweaver–Burk plot for XO-catalyzed steady-state production of uric acid from xanthine, performed by stopped-flow kinetic measurements. The formation of uric acid at 295 nm was monitored at different temperatures at pH 7.1. The straight lines drawn through the points are at 42 °C (●), 37 °C (○), 30 °C (▽), 25 °C (□), 20 °C (△), and 14 °C (◇). The enzyme concentration was 1.1 × 10^{-7} M, and the oxygen concentration was kept constant at 515 μM. The values of the apparent K_m^{Xan} and V_{max} were calculated from the slope and the intercept of the different straight lines.

Table 1: Steady-State and Transient Kinetic Parameters

T (°C)	K_m^{Xan} (μM)	V_{max} (μM min^{-1})	V_{max}/K_m^{Xan} (min^{-1})	k_2 (s^{-1})	K_D (μM)
14	8.3	7.6	0.9	1.4	5
20	7.9	9.4	1.1	2.7	8
25	4.0	15	3.5	8	12
30	5.9	22	3.8	10	14
37	7.7	35	4.5	15	19
42	12	68	5.7	22	22
50	–	–	–	25	26

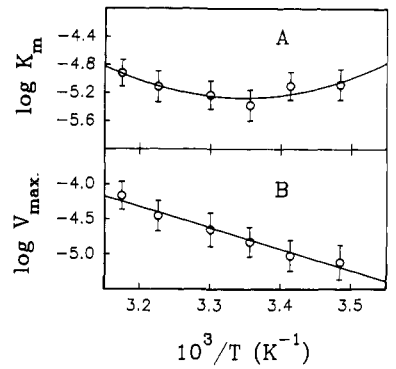

FIGURE 2: Logarithmic plot (A) of K_m^{Xan} against $10^3/T$ for the steady-state conversion reaction of xanthine to uric acid catalyzed by XO at pH 7.1. The logarithmic plot of V_{max} against $10^3/T$ obtained from the same steady-state experiments has been shown in B.

to temperature by the Arrhenius equation. V_{max}, on the other hand, shows a linear variation with temperature (see Figure 2B). The linear dependence of V_{max} on temperature indicates that this velocity is controlled mainly by one composite rate constant, though eq 3 shows that V_{max} depends on both k_2 and k_4. Since V_{max} appears to depend on only one "composite" rate constant, the data in Figure 2B were used to evaluate the corresponding activation energy with the help of the Arrhenius equation, which gives the value of $E_{act}^{V_{max}}$ as 14 kcal/mol. V_{max}/K_m^{Xan} is related to the specificity of the enzyme and was found to increase with temperature (see Table 1). The activation energy obtained from the Arrhenius plot (not shown here) of V_{max}/K_m^{Xan} vs inverse temperature was found to be 11 kcal/mol.

Reductive Half-Reaction of XO with Xanthine. The mechanism of the reductive half-reaction of XO involves the transfer of six electrons to the enzyme in three consecutive steps. Davis *et al.* (1982) and Olson *et al.* (1974b) have

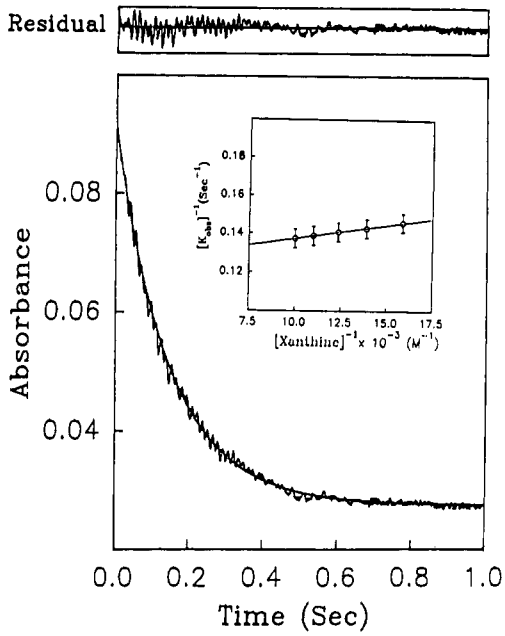

FIGURE 3: Typical stopped-flow trace for the change in absorbance of the anaerobic transient reaction of XO (4.8 μM) with xanthine (63 μM) at pH 7.1 showing the decrease in enzyme absorbance at 450 nm. The line drawn through the experimental trace is the computer fit to the single-exponential function $A_t = A_0 \exp(-kt) + B$, where A_t is the absorbance signal with time, A_0 is the amplitude of the absorbance change, k is the observed rate constant, t is the time in seconds, and B is the equilibrium signal absorbance (offset). Upper curve in the figure: the residual ($A_{obs} - A_{calc}$) plot shows the accuracy of the computer-generated fit. The inset in the figure shows a representative plot of K_{obs}^{-1} of the reductive half-reaction against [xanthine]$^{-1}$. The solid line in the inset through the experimental points is the fit of the experimental data to eq 5.

observed a monophasic decrease in the enzyme absorbance and explained it on the basis of eq 1. We have carried out temperature dependent reductive half-reaction studies at 450 nm for different concentrations of xanthine by stopped-flow technique. The reaction of xanthine with XO decreases the absorbance of the oxidized form of the enzyme at 450 nm. Figure 3 shows the trace of such experiments at 25 °C, which was fitted to a single exponential function to determine the pseudo-first-order rate constant (K_{obs}). The plot of K_{obs}^{-1} vs [Xan]$^{-1}$ gives a straight line, which readily allows determination of the dissociation constant (K_D) and k_2 (see eq 5). One such plot at 25 °C is shown as an inset in Figure 3. Similar studies were carried out at different temperatures, which gave the values of K_D and k_2 between 14 and 50 °C. These values are listed in Table 1. The values of k_2 and K_D have previously been reported at 25 °C (7.7 s^{-1} and 5 μM, respectively, at pH 6.0) (Olson *et al.*, 1974a). Our value of k_2 agrees with the reported one. However, the value of K_D obtained from our measurement is higher than the reported value. This may be due to the difference in pH (7.1 as compared to 6.0 in the reported experiment) in the two measurements. Using the steady-state (K_m^{Xan} and V_{max}) and transient kinetic parameters (K_D and k_2), the rate constants k_1 and k_{-1} were calculated at different temperatures (see eqs 5 and 7), which are listed in Table 2. The thermodynamic parameters (ΔH, ΔS, and ΔG) associated with the binding of xanthine to XO were calculated using eqs 14 and 15 from a linear logarithmic plot of K_D vs $1/T$ (not shown here). ΔH was considered to be temperature independent in the temperature range of the present study (Moratal *et al.*, 1992). The values of ΔH, ΔS, and ΔG were found to be 8.2 kcal/mol, 2.1 cal mol^{-1} deg^{-1}, and 7.6 kcal/mol, respectively. The activation energy calculated from the

Table 2: Microscopic Rate Constants at Various Temperatures

T (°C)	k_1 (M^{-1} s^{-1})	k_{-1} (s^{-1})	k_2' (s^{-1})	k_2'' (s^{-1})
14	2.8×10^5	1.5	82	1.4
20	4.0×10^5	3.3	66	3.6
25	2.3×10^6	28	55	7.4
30	2.6×10^6	35	46	15
37	5.9×10^6	112	37	39
42	8.6×10^6	197	31	76
50	–	–	24	208

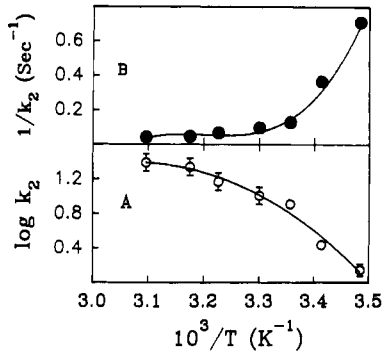

FIGURE 4: Arrhenius plot (A) of the rate constant (k_2) for the dissociation of the enzyme–substrate complex showing nonlinear dependence on inverse temperature. The solid line indicates the trend of the data points. The plot of $1/k_2$ against $1/T$ has been shown in the upper panel (B). The diameter of the circles in B represents the error in data. The solid line through the points is the fit to the experimental data according to eq 10 with A_2' (1.36×10^{-3}), A_2'' (3.61×10^{19}), E_2' (6.3 kcal/mol), and E_2'' (25 kcal/mol). These parameters were used to calculate the rate constants k_2' and k_2''.

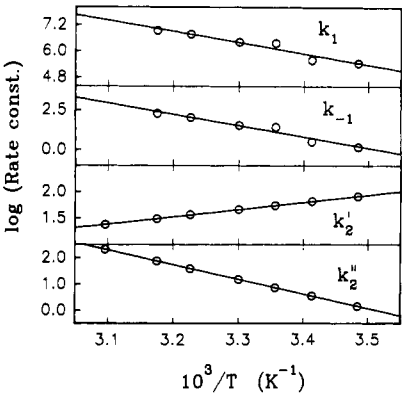

FIGURE 5: Arrhenius plot of the microscopic rate constants showing straight line behavior. The solid lines are fitted through the experimental data points.

logarithmic plot of k_2/K_D against $1/T$ (not shown here) was 6.6 kcal/mol.

The Arrhenius plot of k_2 shows a nonlinear behavior (see Figure 4A). The plot of $1/k_2$ vs $1/T$ shows an interesting behavior (Figure 4B), which was fitted to eq 10 to obtain A_2', A_2'', E_2', and E_2''. The solid line in Figure 4B is the best theoretical fit. The values of A_2', A_2'', E_2', and E_2'' obtained from the fitted curve are 1.36×10^{-3} and 3.62×10^{19} s^{-1} and −6.3 and 25 kcal/mol, respectively. It is noted here that the sign of E_2' and E_2'' are opposite (see also the Discussion). Using these parameters, the values of k_2' and k_2'' were calculated at different temperatures with the help of the Arrhenius rate law. The activation energies for k_1 and k_{-1} were obtained from their linear Arrhenius plots (Figure 5). The values of the activation energies are listed in Table 3. The Arrhenius plots of the individual rate constants have been shown in Figure 5.

Once all these microscopic rate constants were known, eqs 11–13 were used to calculate the thermodynamic parameters

Table 3: Activation Energies[a] Corresponding to Different Rate Constants

k_1	k_{-1}	k_2'	k_2''	k_2/K_D	V_{max}	V_{max}/K_m
22	32	−6.3	25	6.6	14	11

[a] In kcal/mol.

Table 4: Thermodynamic Activation Parameters (Enthalpy, Entropy, and Free Energy) at 25 °C

parameter	$\Delta H^{\ddagger}$ (kcal/mol)	$\Delta S^{\ddagger}$ (cal mol^{-1} deg^{-1})	$\Delta G^{\ddagger}$ (kcal/mol)
k_1	22.6	46	8.7
k_{-1}	32.0	57	15.4
k_2'	−5.7	−70	15.1
k_2''	25.6	31	16.2

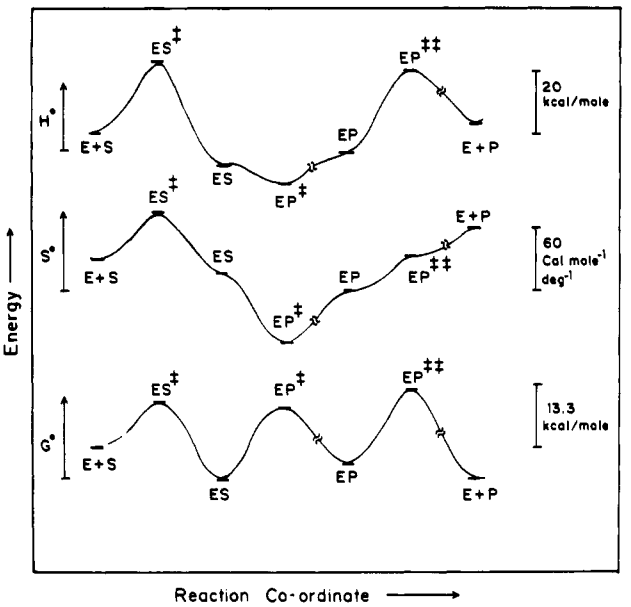

FIGURE 6: Energy profiles showing the changes in standard enthalpy, entropy, and free energy at 25 °C of the different intermediates of the reductive half-reaction of XO. Equations 11–13 were used for calculation of the energy values.

for the activation of individual steps of the reactions. The values of these parameters are listed in Table 4. The energy profiles for the enthalpy, entropy, and free energy at 25 °C are shown in Figure 6. The energies ($\Delta G^{\ddagger}$, $\Delta S^{\ddagger}$, and $\Delta H^{\ddagger}$) of the free enzyme and substrate have been taken as zero in the diagram for convenience. The values of the thermodynamic activation parameters at different temperatures were calculated from the temperature dependence of the rate constant. It was observed that these thermodynamic parameters remain nearly constant with temperature.

DISCUSSION

Steady-State Kinetics. Equation 3 shows that K_m^{Xan} and V_{max} are combinations of several microscopic rate constants. The temperature dependence of the experimentally determined K_m^{Xan} would therefore depend on independent contributions of the temperature dependence of these microscopic rate constants. The expression for K_m^{Xan} can be written as $K_m^{Xan} = (V_{max}E_0)(k_{-1} + k_2)/k_2$. Since V_{max} gives a linear Arrhenius plot with negative slope (Figure 2B), the nonlinear temperature dependence of K_m^{Xan} (Figure 2A) must be attributed to the factor $(k_{-1} + k_2)/k_2$. Since the Arrhenius plot of k_{-1} gives a linear plot with negative slope (Figure 5), the nonlinearity in the Arrhenius plot of K_m^{Xan} must be attributed to k_2.

The Arrhenius plot of V_{max} shows a linear behavior (Figure 2B) which is not apparent from the relation for V_{max} (see eq 3), unless one of the rate constants (k_2 or k_4) is comparatively much smaller. Olson *et al.* (1974a) have shown that $k_4 > k_2$; this could be a reason for the observed linear dependence. The apparent activation energy (14 kcal/mol) calculated from the Arrhenius plot of V_{max} must then correspond to a composite rate constant involving k_2 and k_4.

The concentrations at which the physiological substrates function are generally low and sometimes in the nanomolar region. These concentrations are too low to saturate the enzyme and are negligible compared to their apparent Michaelis constant values. The enzymatic reaction rates under such conditions are closer to V_{max}/K_m^{Xan} rather than to only V_{max}. In other words, this ratio is biologically more relevant to the overall conversion of the substrate to the product. Moreover, the ratio V_{max}/K_m^{Xan} represents the specificity of the enzyme toward its substrates. The increase of this ratio with increasing temperature (data not shown) indicates the decrease in the specificity of the enzyme at higher temperature. It may be due to the temperature dependent change in the thermodynamic parameter of the reaction intermediates. The activation energies calculated for V_{max} and V_{max}/K_m^{Xan} are 14 and 11 kcal/mol, respectively, which indicate that low concentration of xanthine in the biological system decreases the activation barrier toward its conversion to uric acid.

Reductive Half-Reaction of XO. The thermodynamic parameters associated with the binding of xanthine to XO, as derived from the temperature dependence of K_D, show that ΔH (8.2 kcal mol^{-1}), ΔS (2.1 cal mol^{-1} deg^{-1}), and ΔG (7.6 kcal mol^{-1}) are positive. This suggests that the dissociation of the enzyme–substrate complex (XO – xanthine ⇌ XO + xanthine) is an endothermic process. The positive value of enthalpy change may be called "unfavorable" as it is responsible for making free energy change positive (eq 15). The increase in entropy indicates that the dissociation process is mainly an entropy-driven process which is opposed by the unfavorable change in the enthalpy.

The nonlinear Arrhenius plot of k_2 (Figure 4A) indicates involvement of other intermediate species in the breakdown of the enzyme–substrate complex and suggests that k_2 may be composed of other rate constants operative in the mechanism of the reaction. Olson *et al.* (1974) have suggested a two-step breakdown of the enzyme–substrate complex (see eq 8) to explain the results on the time course of the reductive half-reaction. The activation energies for k_2' and k_2'' were obtained by fitting the experimental data of k_2 to eq 10 (Figure 4B). It is obvious from the nature of the curves in Figure 4B that both the activation energies can not be negative. Hence they may either be both positive or have opposite signs. Attempts to fit the experimental data with both the activation energies being positive always gave one of the activation energies as zero (28 and 0.001 kcal/mol). Mcwhirter and Hille (1991) observed that the formation of the different intermediate species of the reductive half-reaction is highly temperature dependent. Since the formation of these intermediates is temperature dependent, the magnitude of the activation energy of any of its microscopic steps can not be zero. Hence, the possibility of both the activation energies being positive can also be ruled out. The observed fit of the experimental data in Figure 4B to the opposite signs of the activation energies is thus a physically meaningful and unique description of the experimental observations. We have taken the magnitude of E_2'' to be positive and that of E_2' to be negative. The positive value of the activation energy may correspond to an elementary

step during the dissociation of the enzyme–substrate complex to the product, but the negative value of the activation energy would be the result of more than one elementary step, corresponding to a composite value of the rate constants. Thus, k_2' is actually the resultant rate constant of more than one elementary step. There is some uncertainty in assigning these two rate constants to the elementary steps of eq 8. The first step in eq 8 involves electron transfer from substrate to the molybdenum center of the enzyme accompanied by concerted nucleophile–hydride transfer from the substrate, whereas the second step represents only the dissociation of the reduced enzyme–product complex (Skibo *et al.*, 1987). Thus the first step is much more complex and may involve additional intermediates. Since the rate constant k_2' may be resolved into more than one intermediate, this rate constant may be assumed to be associated with the first step, *i.e.*, the conversion of $(XO)_{ox}$·Xan → $(XO)_{red}$·urate. The rate constant k_2'' may then be attributed to the last step of the reductive half-reaction ($(XO)_{red}$·urate → $(XO)_{red}$ + urate). These arguments suggest that there should be an intermediate species during the conversion of $(XO)_{ox}$·Xan → $(XO)_{red}$·urate (eq 8). The introduction of an irreversible formation of intermediate within the above conversion reaction as

$$(XO)_{ox}\cdot Xan \xrightarrow{k_l} [(XO)\cdot Xan] \xrightarrow{k_m} (XO)_{red}\cdot urate \quad (16)$$

leads to the following relation:

$$k_2' = \frac{k_l k_m}{k_l + k_m} \quad (17)$$

Since the Arrhenius plot of the calculated k_2' shows straight line behavior (Figure 5), one of these constants has to be negligible with respect to the other. Such a situation will result in only one microscopic rate constant in eq 17. However, since k_2' is a composite rate constant (see above), the mechanism given in eq 16 does not give a complete description of the reaction. If, on the other hand, the mechanism is considered as

$$(XO)_{ox}\cdot Xan \underset{k_{-f}}{\overset{k_f}{\rightleftharpoons}} [(XO)\cdot Xan] \xrightarrow{k_r} (XO)_{red}\cdot urate \quad (18)$$

then the following relation can be obtained

$$k_2' = \frac{k_f k_r}{k_{-f} + k_r} \quad (19)$$

Equation 19 would give a linear Arrhenius plot if $k_{-f} \gg k_r$, which is consistent with the temperature dependence of k_2' (see Figure 5). Thus the mechanism suggested in eq 18 appears to be valid, and k_2' may be a composite rate constant involving k_f, k_{-f}, and k_r. However, these individual rate constants cannot be determined from the present set of experimental data. The apparent activation energies calculated from the Arrhenius plot of k_2' then include three terms due to k_f (E_f), k_{-f} (E_{-f}), and k_r (E_r) which can be equated to $E_f - E_{-f} + E_r$, *i.e.*, $\Delta E_f + E_r$. Since $k_{-f} \gg k_r$, the formation of $(XO)_{red}$·urate from [(XO)·Xan] would involve higher activation energy (E_r, see Figure 7). In order to reach this activation energy level, the species $(XO)_{ox}$·Xan has to first reach [(XO)·Xan], which has higher energy (by ΔE_f) than the former species. With additional energy E_r, the system will reach the activated species [(XO)·Xan]‡, corresponding to the conversion [(XO)·Xan] → $(XO)_{red}$·urate. The situation has been shown in Figure 7.

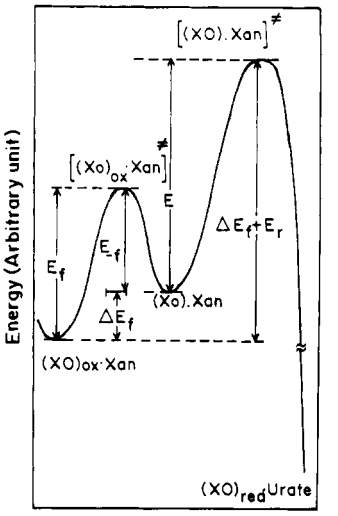

FIGURE 7: Schematic representation of the energy diagram of $(XO)_{ox}$·Xan, (XO)·Xan, and $(XO)_{red}$·urate during the reductive half-reaction.

Microscopic Rate Constants and Their Activation Energies. The rate constants k_1 and k_{-1} were calculated following eq 7. Olson *et al.* (1974b) had calculated $k_1 = 2.0 \times 10^6$ M^{-1} s^{-1} from the steady-state and transient experiments assuming k_{-1} as zero. Our value of k_1 compares favorably with the value of Olson *et al.* (1974b); the small difference could arise from their assumption of k_{-1} being nearly zero. A comparison of the magnitudes of the rate constants for k_1 and k_{-1} indicates very fast attainment of equilibrium during the binding process of xanthine to XO. Since the values of microscopic rate constants k_f and k_{-f} could not be determined here, we have used k_2' for analysis of the thermodynamic parameters of the overall reaction in eq 18. Figure 5 shows that at lower temperatures $k_2' > k_2''$ and at higher temperatures $k_2' < k_2''$. This indicates that the rate-determining step of the reductive half-reaction changes with temperature. This might be due to stabilization of the species [(XO)·Xan] (eq 18) at low temperature, which decreases the magnitude of k_r. The values of the activation energies (Table 3) show that the dissociation of the enzyme–substrate complex (k_{-1}) experiences maximum activation barrier, thus facilitating the conversion of the enzyme–substrate complex to the enzyme intermediates.

Thermodynamic Activation Parameters. The reaction sequence for the formation of the activated complex may be given as below:

$$E + S \rightleftharpoons ES^{\ddagger} \rightleftharpoons ES \rightleftharpoons EP^{\ddagger} \rightarrow EP \rightleftharpoons EP^{\ddagger\ddagger} \rightarrow E + P \quad (20)$$

where E, S, and P represent XO, xanthine, and uric acid, respectively, and the daggered notations refer to the activated complexes. The ES and EP represent the enzyme–substrate ($(XO)_{ox}$·Xan) and the enzyme–intermediate ($(XO)_{red}$·urate) complexes, respectively.

The irreversible mechanisms of the formation of EP and E + P (ES → EP and EP → E + P) (eq 8) do not allow the calculation of energy values for entropy, enthalpy, and free energy of EP and E + P. One of the reasons for this irreversibility may be the high activation barrier for the reverse transformations EP → ES and E + P → EP as compared to their forward reactions. Such a higher activation barrier would arise from a high value of enthalpy of activation (eq 11). The low value of the entropy of activation for the reverse reaction may also make the rate of the backward reaction slow to such

an extent that the reaction becomes virtually irreversible (eq 13). Equation 13 shows that the rate constant would be affected more by the entropy term than by the enthalpy term. Whether the irreversibility of these reactions arises due to both entropy and enthalpy or to only one of them is not clear. Hence for the construction of the energy diagram, we have chosen arbitrary values for EP and E + P.

Figure 6 shows that the formation of the activated complex ($E + S \rightarrow ES^{\ddagger}$), during the substrate-binding process, is an endothermic process. The plot for the free energy also shows that the process is exoergonic and the entropy of activation is positive. $\Delta H^{\ddagger}$ and $\Delta S^{\ddagger}$ contribute to the $\Delta G^{\ddagger}$ in a compensatory manner, which results in a low value of free energy of activation (eq 12). The positive $\Delta G^{\ddagger}$ observed in the present case is due to a very high value of $\Delta H^{\ddagger}$ compared to its entropy of activation. The change in the entropy of activation may arise due to the solvent and structural effects. The solvent effect may involve interaction between the solvent and the reaction system which could change during the course of the reaction. The structural effects refer to the reversible change in the conformation of the enzyme during the course of the reaction. Since xanthine binds to XO at the molybdenum atom, there might be some electrostriction between xanthine and XO which would make the xanthine molecule polar in the enzyme–substrate activated complex. This would result in the abstraction of the solvent molecule, which in the process should decrease the entropy of the system. However, the experimental observation shows that the entropy of activation increases. This anomaly may be due to the transient structural changes in the enzyme associated with the binding of the substrate. The conversion of the activated species to the enzyme–substrate complex ($ES^{\ddagger} \rightarrow ES$) decreases free energy, enthalpy, and entropy. But the conversion of ES to $EP^{\ddagger}$ increases free energy while enthalpy and entropy decrease. It should be recalled that the thermodynamic parameters associated with this step are the summation of other microscopic rates and reflect the character of the overall process. For the conversion of EP to $EP^{\ddagger\ddagger}$, the enthalpy, the free energy, and the change in entropy are positive. One general feature of the reaction sequence (eq 20) is the positive values for the ΔG for all the activated complexes in the forward direction.

CONCLUSION

In the present study, we have examined the mechanism of the reductive half-reaction of XO with xanthine as a substrate. The results of the temperature dependent steady-state and transient kinetic studies have been combined to determine the microscopic rate constants (k_{-1}, k_2', and k_2'') of the half-reaction for the first time. This has also allowed us to evaluate the thermodynamic activation parameters of the microscopic steps involved in the mechanism of the reductive half-reaction. The knowledge of the kinetics and thermodynamics of the microscopic steps of the enzymatic reactions, in general, is limited due to the involvement of the multiple steps in the reaction mechanism, for which the evaluation of microscopic rate constants is difficult. Although catalysis by XO involves multiple steps in its reductive half-reaction, we have been able to describe the thermodynamics and kinetics of the reaction intermediates for the first time from our measurements. Both kinetic and thermodynamic parameters of the intermediates in the present report are due to the interactions of physiological substrate xanthine with XO; thus all these parameters are directly relevant toward the mechanism of action of the enzyme. It is also interesting to note that the change in temperature alters the rate-determining step of the half-reaction. The conversion reaction of the enzyme–substrate complex to the enzyme–product complex (k_2') is the rate-limiting step at higher temperature; however, at lower temperature, the dissociation of the enzyme–product complex (k_2'') is the rate-limiting step. Our results suggest the existence of three molecular intermediates during the reductive half-reaction. The rate constant k_2' refers to electron transfer from the substrate to the enzyme and to the subsequent concerted nucleophile–hydride transfer from the substrate. Hille and Anderson (1991) have shown that the rates of intramolecular electron transfer among the redox active centers are fast (>90 s^{-1} at 20 °C). However, the magnitudes of k_2' and k_2'' obtained from our study are lower than those of the intramolecular electron-transfer rate. This indicates that these rate constants (k_2' and k_2'') are also associated with the involvement of bond-breaking and bond-making steps of the reductive half-reaction. It has been observed from the EPR studies that at low pH (<7.5) the intensity of the "very rapid EPR signal" is small (Edmondson *et al.*, 1973). Hille and Anderson (1991) have ascribed this low intensity to the direct release of uric acid from the Mo(IV)·urate complex. Hence the species described as XO_{red}·urate in the present paper would refer to the Mo(IV) complex of the enzyme with urate. Since the XO_{ox}·xanthine complex is formed due to the interaction of xanthine with the oxidized enzyme, it can be represented as Mo(VI)·xanthine. McWhirter and Hille (1991) have discussed the reductive half-reaction on the basis of single-step conversion of the Mo(VI)·substrate complex to the Mo(IV)·product complex and indicated that another intermediate may be involved during this conversion reaction. The results from our experiment suggest that there may be an intermediate species between the above two complexes which has been represented here as 'XO·Xan' (see eq 18). The two different processes occurring in the conversion of Mo(VI)·xanthine to Mo(IV)·urate are the electron transfer and the bond breaking/bond making. Since the electron-transfer rates are faster than the bond-breaking/bond-making processes, it is likely that these two conversions will occur through the two different processes giving rise to two different intermediates. The rate constant k_2' corresponds to $k_f k_{-f}/k_r$. Skibo *et al.* (1987) have shown that the bond-breaking and bond-making processes of the enzyme–substrate complex make partial negative charge in the substrate and this partial negative charge facilitates the electron transfer from the substrate to the molybdenum atom. On the basis of the above discussion, we are tempted to suggest that the species "XO·Xan" may arise due to the bond breaking and bond making of xanthine in the enzyme–substrate complex without any electron transfer from xanthine to molybdenum. Thus, the conversion of (XO)·Xan to $(XO)_{red}$·urate may involve electron transfer from the substrate to the oxidized Mo(VI) atom.

ACKNOWLEDGMENT

We thank Dr. G. Krishnamoorthy for helpful suggestions and discussions.

REFERENCES

Bray, R. C. (1975) in *The Enzymes* (Boyer, D. P., Ed.) Vol. XII, Part B, pp 300–419, Academic Press, New York.

Bray, R. C. (1980) in *Biological Magnetic Resonance* (Berliner, L. J., & Reuben, J., Eds.) pp 45–84, Plenum, New York.

Bray, R. C. (1988) *Q. Rev. Biophys. 21*, 299–329.
Bray, R. C., Palmer, G., & Beinert, H. (1964) *J. Biol. Chem. 239*, 2667–2676.
Bray, R. C., Gutteridge, S., Stotter, D. A., & Tanner, S. J. (1979) *Biochem. J. 177*, 357–360.
Bunting, J. W., & Gunasekara, A. (1982) *Biochim. Biophys. Acta 704*, 444–449.
D'Ardenne, S. C., & Edmondson, D. E. (1990) *Biochemistry 29*, 9046–9052.
Davis, M. D., Olson, J. S., & Palmer, G. (1982) *J. Biol. Chem. 257* (24), 14730–14737.
Davis, M. D., Olson, J. S., & Palmer, G. (1984) *J. Biol. Chem. 259* (6), 3526–3533.
Edmondson, D., Massey, V., Palmer, G., & Beachan, L. M. (1972) *J. Biol. Chem. 247*, 1597–1640.
Edmondson, D., Ballou, D., Van Heuvelen, A., Palmer, G., & Massey, V. (1973) *J. Biol. Chem. 248*, 6135–6144.
Escribano, J., Garcia-Canovas, F, & Garcia-Carmona, F. (1988) *Biochem. J. 254*, 829–833.
Hille, R., & Massey, V. (1985) in *Molybdenum Enzymes* (Spiro, T. G., Ed.) pp 443–518, John Willey and Sons, New York.
Hille, R., & Anderson, R. F. (1991) *J. Biol. Chem. 266* (9), 5608–5615.
Hille, R., & Massey, V. (1991) *J. Biol. Chem. 266* (26), 17401–17408.
Hille, R., Hagen, W. R., & Dunham, W. R. (1985) *J. Biol. Chem. 260* (19), 10569–10575.
Hille, R., George, G. N., Eidsness, M. K., & Cramer, S. P. (1989) *Inorg. Chem. 28*, 4018.
Jezewska, M. M. (1973) *Eur. J. Biochem. 36*, 385–390.
Kim, J. H., & Hille, R. (1993) *J. Biol. Chem. 268* (1), 44–51.
King, E. L., & Altman, C. (1956) *J. Phys. Chem. 60*, 1375–1378.
Komai, H., Massey, V., & Palmer, G. (1969) *J. Biol. Chem. 244*, 1692–1700.
Kramer, S. P., Johnson, J. L., Rebeiro, A. A., Millington, D. S., & Rajagopalan, K. V. (1987) *J. Biol. Chem. 262* (34), 16357–16363.
Lineweaver, H., & Burk, D. (1934) *J. Am. Chem. Soc. 56*, 658–656.
Massey, V., & Edmondson, D. (1970) *J. Biol. Chem. 245*, 6595–6598.
Massey, V., Brumby, P. E., Komai, H., & Palmer, G. (1969), *J. Biol. Chem. 244*, 1682–1691.
McWhirter, R. B., & Hille, R. (1991) *J. Biol. Chem. 266* (35), 23724–23731.
Moratal, J. M., Martinez-Ferrer, M. J., Donaire, A., & Aznar, L. (1992) *J. Inorg. Biochem. 45*, 65–71.
Morpeth, F. F. (1983) *Biochim. Biophys. Acta 744*, 328–324.
Olson, J. S., Ballou, D. P., Palmer, G., & Massey, V. (1974a) *J. Biol. Chem. 249* (14), 4350–4362.
Olson, J. S., Ballu, D. P., Palmer, G., & Massey, V. (1974b) *J. Biol. Chem. 249*, 4363–4382.
Radi, R., Tan, S., Prodanov, E., Evans, R. A., & Parks, D. A. (1992) *Biochim. Biophys. Acta 1112*, 178–182.
Rubbo, H., Radi, R., & Prodanov, E. (1991) *Biochim. Biophys. Acta 1074*, 386–391.
Skibo, E. B. (1986) *Biochemistry 25* (15), 4189–4194.
Skibo, E. B., Gilchrist, J. H., & Lee, C. H. (1987) *Biochemistry 26* (11), 3032–3037.
Wilson, G. L., Greenwood, R. J., Pilbrow, J. R., Spence, J. T., & Wedd, A. G. (1991) *J. Am. Chem. Soc. 113*, 6803–6812.